Journal of Material Sciences & Engineering

Abbad et al., J Material Sci Eng 2013, 2:3
DOI: 10.4172/2169-0022.1000127

Research Article Open Access

# Removal of Methylene Blue from Coloured Effluents by Adsorption onto ZnAPSO-34 Nanoporous Material

**Abbad B, Lounis A*, Taibi K and Azzaz M**

*Laboratory of Sciences and Material Engineering, USTHB, BP 32 El Alia, Algeria*

**Abstract**

The effluents of wastewater in some industries such as, textiles, leather, paper and plastics contain various kinds of synthetic dyes. Molecular sieves like aluminosilicate or aluminophosphate materials containing tiny pores of precise and uniform size, which are used as adsorbents, catalyst carriers, desiccants, and so on. In this work, initial dye concentration, contact time, adsorbent dosage, pH and kinetic studies were carried out to evaluate the adsorption capacity ZnAPSO-34 nanoporous material for the removal of MB from aqueous solutions. The results showed that ZnAPSO-34 could be employed as an alternative for the removal of dyes and colors from aqueous solutions.

**Keywords:** Waste treatment; Clean processing techniques; Environmental materials

## Introduction

The growth of the world population in the last century, in addition with economic growth , the development of various industries and the use of fertilizers and pesticides in modern agriculture, have generated a significant quantity of hazardous waste, reflected in a considerable rise in both fresh water consumption and wastewater production. The effluents of wastewater in some industries such as dyestuff, textiles, leather, paper and plastics contain various kinds of synthetic dyestuffs [1]. The textile industry which is one of the largest water consumer in the world, produces wastewater comprising various recalcitrant agents such as dye, sizing agents and dying aid. Removal of emerging contaminants of concern is now as ever important in the production of safe drinking water and the environmentally responsible release of wastewater. There are many conventional methods that can remove colored dyes from wastewater: chemical coagulation-flocculation, membrane technology, biological methods such as anaerobic⁄aerobic sequential processes, oxidative degradation by using chlorine or ozone, photo-degradation, and adsorption [2]. The As synthetic dyes in wastewater cannot be efficiently decolorized by traditional methods, the adsorption of synthetic dyes on inexpensive and efficient solid supports was considered as a simple and economical method for their removal from water and wastewater. Hence, coloured wastewater treatment requires new adsorbents that are economical, easily available and effective. There are several types of adsorbent being applied in industrial wastewater such as activated carbon, silica gel and alumina [3]. Molecular sieves like aluminosilicate or aluminophosphate materials containing tiny pores of precise and uniform size, which are used as adsorbents, catalyst carriers, desiccants, and so on. Among the AlPOs, the metalloaluminophosphates (MAPO) and metallosilicoaluminophosphates (MAPSO) materials encompass the characteristics of both zeolites and aluminophosphates, which results in their unique catalytic, ion-exchange and adsorbent properties [4]. ZnAPSO-34 is a synthetic aluminophosphate materials with the chabazite (CHA) structure [5]. The pore structure comprises eight member rings with 0.38 nm opening into large ellipsoidal cavities of 0.67-1.0 nm. In this work, initial dye concentration, contact time, adsorbent dosage, pH and kinetic studies were carried out to evaluate the adsorption capacity ZnAPSO-34 nanoporous material for the removal of MB from aqueous solutions.

## Materials and Methods

### Preparation

ZnAPSO-34 was synthesized by following previously reported procedure [6]. The typical synthesis gels with a molar composition of 0.8SiO2:0.8Al2O3:1- P2O5:1TEAOH:0.4Zn:225H2O were prepared in 120 ml Teflon-lined autoclave. Isopropoxyde of alumina (Fluka) and ortho-phosphoric acid (Merck 85%) were used as aluminum and phosphorus sources, respectively; the divalent metal was introduced as acetate (zinc acetate, Fluka p.a.), other reactants were fumed silica (Aerosil 200, Serva), tetraethylammonium hydroxide (20% aqueous solution, Fluka) and deionized water.

In order to obtain the final gel solution Isopropoxyde of alumina was slowly added to an aqueous solution containing ortho-phosphoric acid and the metal salt, maintaining the mixture under magnetic stirring for 1h. The TEAOH solution, followed by the addition of the required amount of silica was mixed. After the addition of the silica, the solution was maintained under stirring 2 h.

The crystallization occurred under static conditions in an oven at 180-200°C for 24h. The autoclaves were cooled down to room temperature under running water, and the products were recovered by centrifugation, washed and dried at 80°C overnight.

The final product was a white powder. Finally, the product was calcined at 550°C for 5 h at the rate of 1°C/min to remove the organic templates.

### Preparation of basic dye solution

Methylene Blue used was of analytical reagent grade and supplied by BIOCHEM Chemopharma (MW=319.86g, Absorption max

***Corresponding author:** A. Lounis, Laboratory of Sciences and Material Engineering, USTHB, BP 32 El Alia, Algeria, E-mail: zlounis@yahoo.com

**Received** August 07, 2013; **Accepted** September 20, 2013; **Published** September 25, 2013

**Citation:** Abbad B, Lounis A, Taibi K, Azzaz M (2013) Removal of Methylene Blue from Coloured Effluents by Adsorption onto ZnAPSO-34 Nanoporous Material. J Material Sci Eng 2: 127. doi:10.4172/2169-0022.1000127

(water):663-667 nm). Stock solutions of the test reagent were made by dissolving Methylene Blue, (3,9-bis dimethyl- aminophenazo thionium chloride), in distilled water. The structure of this dye is shown in Figure 1.

All the other chemicals used were of analytical reagent grade and were purchased from Merck (Germany).

## Batch sorption studies

**Adsorption studies:** The adsorption was performed by batch experiments. Kinetic experiments were carried out by stirring 250 ml of dye solution of known initial dye concentration with 0.05 g of ZnAPSO-34 at room temperature (20°C) at 400 rpm in different 500 ml PE flasks. At different time intervals, samples have been drawn out and then centrifuged at 3500 rpm for 10 min. The concentration in the supernatant solution was analyzed using a UV spectrophotometer SHIMADZU 1800 by measuring absorbance at λ max = 664 nm and pH = 6. Adsorption isotherms were carried out by contacting 0.05 g of ZnAPSO-34 with 250ml of methylene blue over the concentration ranging from 2 to 10 mg $l^{-1}$.

The effect of pH was observed by studying the adsorption of dye over a pH range of 2-10. The initial pH of the dye solution was adjusted by the addition of 0.1 N solution of hydrogen chloride (HCl) or sodium hydroxide (NaOH).

The amount of dye adsorbed per unit weight of adsorbent; qt (mg.g.$1^{-1}$) was calculated using the mass balance equation given by:

$$q_t = \frac{(C_0 - C_t)V}{m} \quad (1)$$

where, $C_0$ (mg/l) is the initial dye concentration, $C_t$ (mg/l) is the liquid phase concentrations of dye at any time, V is the volume of the solution (l) and m is the mass of dry adsorbent used (g).

The dye removal percentage can be calculated as follows:

$$R(\%)_t = \frac{(C_0 - C_t)}{C_0}100 \quad (2)$$

Due to the inherent bias resulting from linearization of the isotherm model and kinetic model, the non-linear regression Root Mean Square Error (RMSE) test was employed as criterion for the quality of fitting. The RMSE of a model is evaluated by error analysis.

**Error analysis:** Because of the inherent bias resulting from the linearisation of the isotherm and kinetic models, four different error functions of the non-linear regression basin were employed as criteria for the quality of fitting [7].

**The RMSE:** The RMSE has been used by a number of researchers in the field to test the adequacy and accuracy of the model fit with the experimental data:

$$RMSE = \sqrt{\frac{1}{n-2}\sum_{1}^{n}(q_i - q_{ie})^2} \quad (3)$$

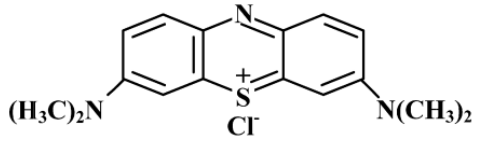


**Figure 1:** The structure of methylene blue.

where $q_i$ is the experimental sorption capacity from the batch experiment i, $q_{ie}$ is the sorption capacity estimated from the sorption model for corresponding $q_i$ and n is the number of observations in the batch experiment.

**The chi-square test:** The chi-squared test statistic is basically the sum of the squares of the differences between the experimental data and data obtained by calculating from models, with each squared difference divided by the corresponding data obtained by calculating from models. The chi-squared test has some similarity with the root mean square error and is given as:

$$\chi^2 = \sum_{i=1}^{n}\frac{(q_i - q_{ie})^2}{q_{ie}} \quad (4)$$

**The sum of the absolute errors:** The sum of the absolute errors (SAE) is given as:

$$SAE = \left|\sum_{i=1}^{n}|q_t - q_{i.e}\right| \quad (5)$$

The isotherm parameters determined by this method provide a better fit as the magnitude of the errors increase, biasing the fit towards the high concentration data.

**The average relative error:** The average relative error (ARE) is defined as:

$$ARE = \frac{100}{n}\sum_{i=1}^{n}\left|\frac{q_t - q_{i.e}}{q_t}\right| \quad (6)$$

This error function attempts to minimise the fractional error distribution across the entire concentration range.

## Characterization of the adsorbent

The as-synthesized product was characterized initially by X-ray powder diffraction using a diffractometer (Miniflex2, RIGAKU) equipped with a linear position sensitive detector (CuKa1 radiation, k = 1.5406Å). The morphology and average size of the crystals were determined by Scanning Electron Microscopy (SEM) using a HITACHI S4800 microscope.

Elemental composition of the products (Al, P, Si, Zn ) was determined by using JEOL 5800 SEM with energy dispersive X-ray analyser attachment (EDX).

# Results and Discussion

## Cristallinity

The examination of the powder data of the sample revealed that only one phase was identified, which correspond to Chabazite structure [8]. The XRD patterns (Figure 2) illustrate the rather high crystallinity of all samples. No extra peak related to transition metal oxides appeared, indicating the purity of the products.

## Morphology and crystal size

We have observed the sample by SEM, looking for the morphology of the crystals. SEM images of the calcined samples are provided in Figure 3. The sample prepared shows the typical Chabazite morphology: cubic crystals are well-developed in the size range of 3-10µm. Particles of cubic morphology (1-5µm in size) form ball-shaped aggregates.

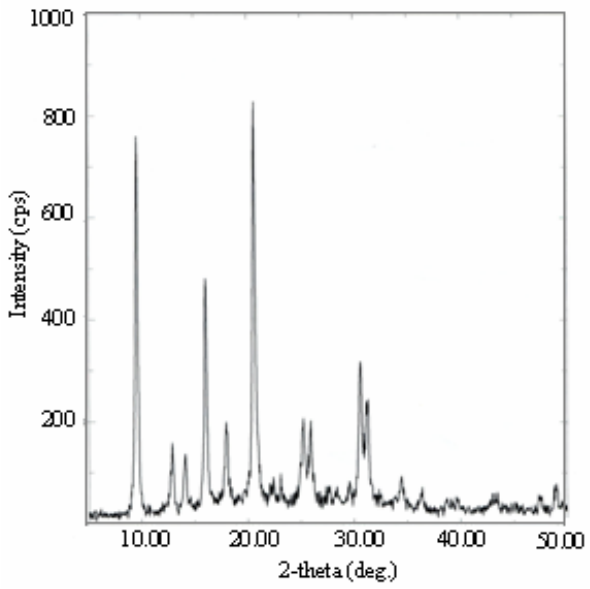


**Figure 2:** X-ray patterns of ZnAPSO-34 calcined at 500°C.

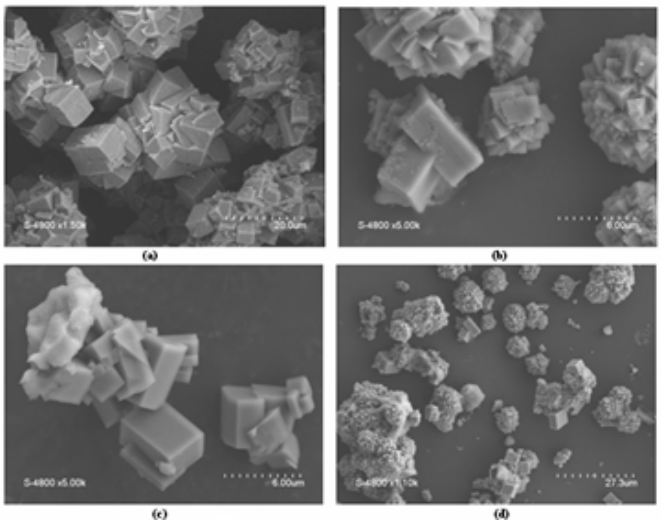


**Figure 3:** (a-d) SEM mocrographs of ZnAPSO-34 at different magnifications.

## Elemental analysis

The SEM-EDAX data were measured randomly across different crystals and in different areas on different crystal. The presence of elemental Zn, on the cubic surface of the ZnAPSO-34 crystallites, was confirmed by using the EDX technique and the result is shown in Figure 4.

## Thermal analysis

Figure 5 shows the TG and DTA results of the product measured after synthesis. ZnAPSO-34 exhibited a weight loss of 7.3% at temperature less than 200°C due to the loss of adsorbed water.

The endothermic peak in the corresponding ATD curve proved that TEAOH was thermally decomposed near 450°C. TG/DTG analyses of as-synthesized ZnAPO-34 samples indicate that physically adsorbed water is expelled in the 120-230°C temperature range, whereas the main decomposition of the template (TEA+cations) occurs between 400 and 600°C, in agreement with previous observations.

## Effect of various parameters on the MB Adsorption

**Effect of adsorbent dose:** The effects of adsorbent dosage on MB removal are presented in Figure 6. Removal efficiency increased from 85% to 94% with an increase in the dosage from 0.05 to 0.1 g. $l^{-1}$, and then remained almost constant. This was caused by the fact that, with increasing adsorbent dosage, more adsorption sites are available. However, increasing the sites had little effect on removal efficiency at high adsorbent dosage because of the establishment of equilibrium at an extremely low adsorbate concentration in the solution before reaching saturation. It can also be seen from Figure 6 that the MB removal efficiency changed slightly from 85% to 97% with an increase in adsorbent dosage from 0.1 to 0.25g $l^{-1}$. This result is mainly because the adsorption sites were more or less saturated by MB at low adsorbent doses (<0.1 g $l^{-1}$), but unsaturated at high doses (>0.25 g $l^{-1}$). The adsorbent dosage was fixed at 0.05 g $l^{-1}$ for the remaining experiments.

As can be seen from Figure 7, the correlation coefficient, $R^2$ of

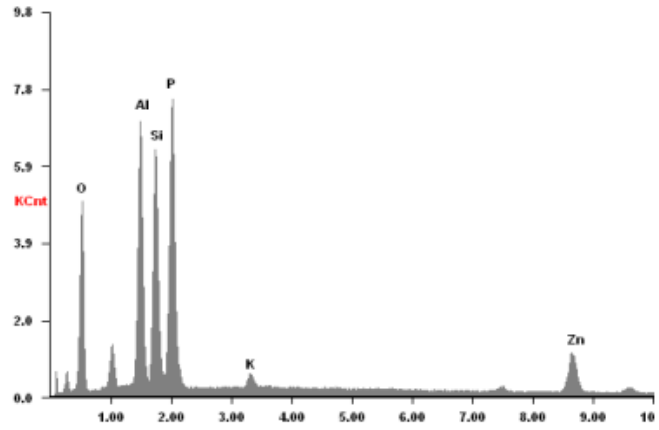


**Figure 4:** EDX results in the analysis of ZnAPSO-34.

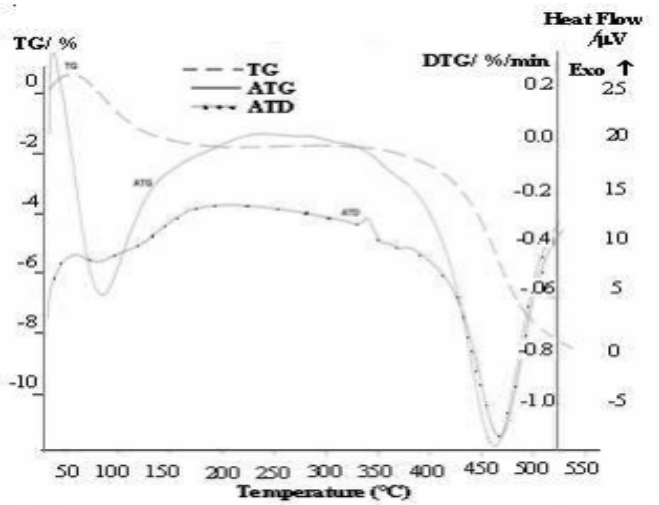


**Figure 5:** The TG-DTA curves of ZnAPSO-34.

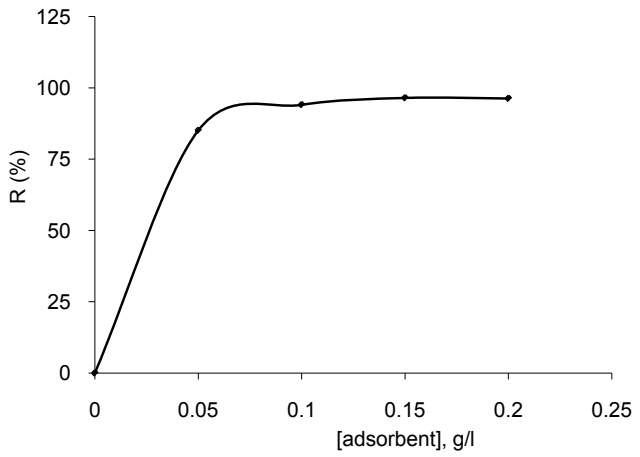


**Figure 6:** Effect of adsorbent dosage on the adsorption of Metlylene Blue onto ZnAPSO-34 (dye concentration: 2mg.l$^{-1}$ Temperature=293 K; contact time= 300 min), pH=6.

pseudo-second-order kinetic model were greater than 0.99 for both MB solutions. Therefore, the calculated $q_e$ values agreed with the experimental $q_e$ values, implying that the adsorption kinetic of MB is well described by pseudo-second-order model.

**Adsorption kinetics:** The following expressions were used to describe two models, respectively:

$$\ln(q_e-q_t)=\ln(q_e)-k_1 t \quad (7)$$

$$\frac{t}{q_t}=\frac{t}{q_e}+\frac{1}{k_2.q_e^2} \quad (8)$$

where $q_t$ and $q_e$ are the amount of MB adsorbed on the adsorbents (mg·g$^{-1}$) at time t and at equilibrium, respectively $k_1$ (min$^{-1}$) and $k_2$ (g·mg$^{-1}$·min$^{-1}$) are the rate constants of first order and second order, respectively.

From Table 1, it can be seen that the pseudo-second order kinetic rate constants decreased with the increasing of initial MB concentrations. This is due to the competition for the adsorbent active sites are increased at higher concentration and consequently the adsorption rate will become slower. According to the kinetic modelling results shown in Table 2, the correlation coefficient for the pseudo-second-order model obtained were greater than 0.9999 for all concentrations, in order to compare the validity of pseudo second-order model more definitely a RMSE and $\chi^2$ are calculated. Again $q_e$ should equal the experimentally obtained equilibrium capacity for this model to be valid. The calculated $q_e$ values also agree very well with the experimental data. These indicate that the adsorption system studied belongs to the second-order kinetic model, suggesting that chemisorption might be the rate-limiting step that controlled the adsorption process. It could be presumed that the pseudo-second-order equation was used to describe chemisorption involving valency forces through the sharing or exchange of electrons between the adsorbent and adsorbate as covalent forces, and ion exchange.

**Adsorption isotherms:** Adsorption isotherms are critical in optimizing the use of adsorbents and describe how adsorbate interacts with adsorbent. The analysis of the isotherm data with either theoretical or empirical equations is important to develop an equation which accurately represents the results and which could be used for design [9]. Several isotherms equations are available. Three of them have been selected in this study: Langmuir, Temkin and Freundlich isotherms.

**Langmuir isotherm:** The Langmuir adsorption isotherm has been successfully applied to many pollutants adsorption processes and has been the most widely used sorption isotherm for the sorption of a solute from a liquid solution [10]. The saturated monolayer isotherm can be represented as

$$q_e = q_{\max}\frac{bC_e}{1+bC_e} \quad (9)$$

The above equation can be rearranged to the common linear form (Figure 8):

$$\frac{C_e}{q_e}=\frac{C_e}{q_{\max}}+\frac{1}{bq_{\max}} \quad (10)$$

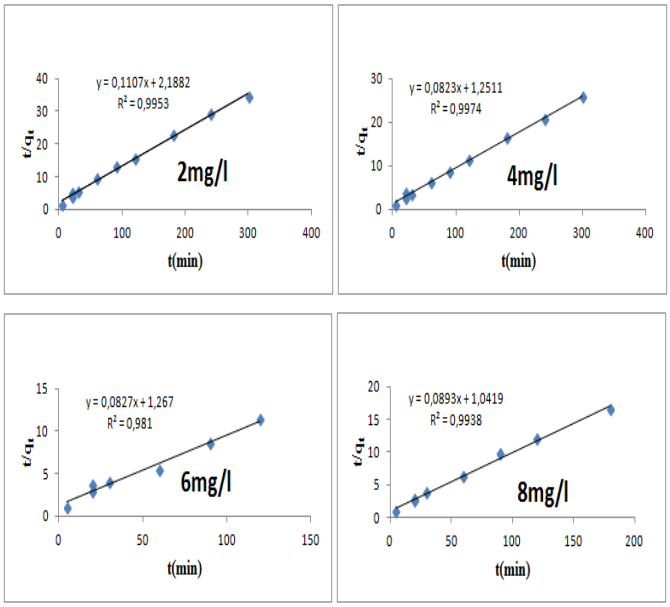


**Figure 7:** Pseudo second order plot of the effect of initial MB concentration (mg/l) on the sorption of MB by ZnAPSO-34.

| Models | Concentration BM mg/l Parameters | 2 | 4 | 6 | 8 |
|---|---|---|---|---|---|
| Pseudo-second-order | $R^2$ | 0.995 | 0.997 | 0.981 | 0.999 |
| | $k_2$ (g.mg$^{-1}$ min$^{-1}$) | 5.97 10$^{-3}$ | 5.88 10$^{-3}$ | 4.1810$^{-3}$ | 5.06 10$^{-3}$ |
| | $q_e$ cal (mg g$^{-1}$) | 8.775 | 11.728 | 13.101 | 14.238 |
| | $q_e$ exp (mg g$^{-1}$) | 8.75 | 11.66 | 13.73 | 13.78 |
| | h (mg g$^{-1}$min$^{-1}$) | 0.457 | 0.799 | 0.789 | 0.96 |
| | $IR_{50}$ (mg g$^{-1}$) | 1.169 | 1.173 | - | 0.96 |
| | $IR_{80}$ (mg g$^{-1}$) | 0.094 | 0.094 | - | 0.077 |
| | $t_{½}$ (min) | 3.025 | 5.604 | - | 10.297 |
| | $\chi^2$ | 0.023 | 0.053 | - | 0.203 |
| | RMSE | 0.197 | 0.4 | - | 0.876 |
| Pseudo-first-order | $R^2$ | 0.98 | 0.976 | 0.96 | 0.972 |
| | $k_1$ (g.mg$^{-1}$ min$^{-1}$) | 0.028 | 0.039 | 0.054 | 0.066 |
| | $q_e$ cal (mg g$^{-1}$) | 8.75 | 11.66 | 13.73 | 13.78 |
| | $\chi^2$ | 7.438 | 6.356 | 5.782 | 8.505 |
| | RMSE | 1.089 | 1.326 | 2.618 | 3.131 |

**Table 1:** Kinetic parameters for the adsorption of MB on ZnAPSO-34.

| Models / Parameters | Langmuir | Temkin | Freundlich |
|---|---|---|---|
| $\chi^2$ | 0.175 | 6.978 | 0.045 |
| $R^2$ | 0.997 | 0.96 | 0.975 |
| $q_{max}$ (mg.g$^{-1}$) | 14.49 | - | - |
| b (l.mg$^{-1}$) | 4.059 | 1.867 | - |
| $R_L$ | 0.046 | | |
| $K_f$ (mg$^{1-1/n}$g$^{-1}$l$^{1/n}$) | - | - | 10.8 |
| 1/n | - | - | 0.168 |
| $K_T$ (l.mg$^{-1}$) | - | 6.64 $10^{-4}$ | - |
| $b_T$ (J.mol$^{-1}$) | - | - | - |
| $K_E$ (l.mg$^{-1}$) | - | - | - |
| SAE | 2.15 | 21.82 | 1.21 |
| ARE | 0.848 | 5.08 | 0.369 |
| RMSE | 0.93 | 7.8 | 0.553 |

**Table 2:** Isotherm parameters for the adsorption of Methylene blue on ZnAPSO-34.

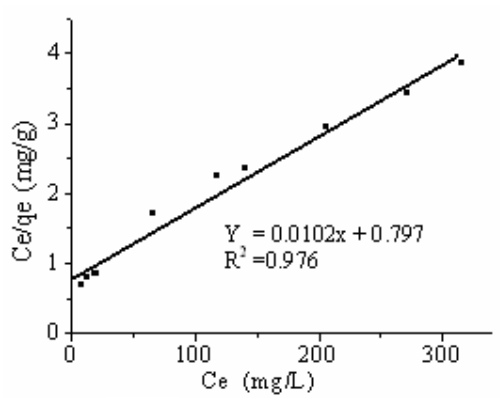


**Figure 8:** Langmuir isotherm plot.

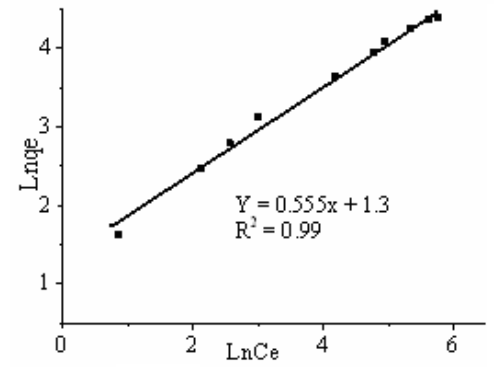


**Figure 9:** Freundlich isotherm plot.

where $C_e$ is the equilibrium concentration (mg l$^{-1}$); $q_e$ is the amount of MB adsorbed per unit mass of zeolite (mg g$^{-1}$).

**Temkin isotherm:** The derivation of the Temkin isotherm assumes that the fall in the heat of adsorption is linear rather than logarithmic, as implied in the Freundlich equation. The Temkin isotherm [11].

$$q_e = \frac{RT}{b_T}\ln(K_T.Ce) \quad (11)$$

$q_{max}$ is $q_e$ for a complete monolayer (mg.g$^{-1}$), a constant related to sorption capacity; and b is a constant related to the affinity of the binding sites and energy of adsorption(l.mg$^{-1}$). From Table 2 it can be observed that the calculated isotherm parameters and their corresponding RMSE, ARE, SAE and $\chi^2$ values vary for the three linearized types of isotherms. It can be seen that the Freundlich model yields a better fit than the Langmuir and Temkin model, as reflected by a RMSE, and $\chi^2$ values. Freundlich isotherm showed better fit followed by langumuir isotherms.

Where, R (J/mol.K) is the gas constant, T (K) the absolute temperature, $b_T$ (J.mol-1) constant related to the heat of adsorption and $K_T$ is Temkin constant (L/mg).

**Freundlich isotherm:** Freundlich isotherm is an empirical equation describing adsorption onto a heterogeneous surface (Figure 9). The Freundlich isotherm [12] is commonly presented as

$$q_e = K_f C_e^{1/n} \quad (12)$$

where $K_f$ and n are the Freundlich constants related to the adsorption capacity and adsorption intensity of the sorbent, respectively. Eq. (12) can be linearized by taking logarithms:

$$\ln q_e = \ln K_f + 1/n \ln C_e \quad (13)$$

The essential feature of the Langmuir isotherm can be expressed by means of '$R_L$', a dimensionless constant referred to as separation factor or equilibrium parameter [13]. $R_L$ is calculated using the following equation

$$R_L = \frac{1}{1+bC_0} \quad (14)$$

where $C_0$ is the highest initial dye concentration (mg.L$^{-1}$) and b (L/mg) is Langmuir constant. The value of $R_L$ calculated as above equation is incorporated in Table 2. The value of $R_L$ indicated the type of isotherm to be irreversible ($R_L$=0), favourable (0<$R_L$<1), linear ($R_L$=1) or unfavourable ($R_L$>1). Further, the $R_L$ value for MB onto ZnAPSO-34 at 20°C is 0.046 and therefore, its adsorption is favourable.

## Conclusions

From this study, the ability of ZnAPSO-34 to remove Methylene blue from aqueous solution was investigated. We can conclude that the analysis by SEM and EDX showed that the adsorbent material has a micro porous structure and it consists mainly of Al, P, Si and Zn. The equilibrium adsorption isotherms have been validated in detail by Langmuir and Freundlich and Temkin models. Equilibrium data fitted very well in the Langmuir isotherm equation, confirming the monolayer adsorption capacity of methylene blue onto ZnAPSO-34 with a monolayer adsorption capacity of 14.49 mg/g. The conditioning time of 3h was found to be sufficient for reaching equilibrium. The results obtained confirm that ZnAPSO-34 can remove Methylene blue from aqueous solution. The results also showed that the process follows pseudo second-order kinetics. The low values of maximum adsorption capacities obtained from Langmuir model, confirm that the molecule of MB is not strongly adsorbed inside the pores because of its size. Only the surface functions are responsible for adsorption.

### References

1. Forgacs E, Cserhati T, Oros G (2004) Removal of synthetic dyes from wastewaters: A review. Environ Int 30: 953-971.
2. Yavuz O, Aydin AH (2006) Removal of direct dyes from aqueous solution using various adsorbents. Pol J Environ Stud 15: 155-161.
3. Rafatullah M, Sulaiman O, Hashim R, Ahmad A (2010) Adsorption of methylene blue on low-cost adsorbents: A review. J Hazard Mater 177: 70-80.

4. Gonzalez G, Pina C, Jacas A, Hernandez M, Leyva A (1998) Synthesis and characterization of ZnAPO-34 molecular sieve with CHA structure type. Micropor Mesopor Mater 25: 103-108.
5. http://www.sciencedirect.com/science/book/9780444530646
6. Tusar NN, Kaucic V, Geremia S, Vlaic G (1995) A zinc-rich CHA-type aluminophosphate. Zeolites 15: 708-713.
7. Han R, Wang Y, Zou W, Wang Y, Shi J (2007) Comparison of linear and nonlinear analysis in estimating the Thomas model parameters for methylene blue adsorption onto natural zeolite in fixed-bed column. J Hazard Mater 145: 331-335.
8. http://www.iza-structure.org/databases/books/Collection_4ed.pdf
9. McKay G, Bino MJ, Altamemi AR (1985) The adsorption of various pollutants from aqueous solutions on to activated carbon. Water Res 19: 491-495.
10. Langmuir I (1918) The adsorption of gases on plane surfaces of glass, mica and platinum. J Am Chem Soc 40: 1361-1403.
11. Temkin MJ, Pyzhev V (1940) Recent modifications to Langmuir isotherms. Acta Physicochim 12: 21-22.
12. Freundlich MF (1906) Over the adsorption in solution. J Phys Chem 57: 385-470.
13. Hall KR, Eagleton LC, Acrivos A, Vermeulen T (1966) Pore- and solid-diffusion kinetics in fixed-bed adsorption under constant-pattern conditions. Ind Eng Chem Fundam 5: 212-223.